



*Citation for published version:*

Blackaby, WJM, Neale, SE, Isaac, CJ, Sabater, S, MacGregor, SA & Whittlesey, MK 2019, 'N-Heterocyclic Carbene Non-Innocence in the Catalytic Hydrophosphination of Alkynes', *ChemCatChem*, vol. 11, no. 7, pp. 1893-1897. <https://doi.org/10.1002/cctc.201900220>

*DOI:*

[10.1002/cctc.201900220](https://doi.org/10.1002/cctc.201900220)

*Publication date:*

2019

*Document Version*

Peer reviewed version

[Link to publication](#)

This is the peer reviewed version of the following article: W. J. M. Blackaby, S. E. Neale, C. J. Isaac, S. Sabater, S. A. Macgregor, M. K. Whittlesey, *ChemCatChem* 2019, 11, 1893., which has been published in final form at [10.1002/cctc.201900220](https://doi.org/10.1002/cctc.201900220). This article may be used for non-commercial purposes in accordance with Wiley Terms and Conditions for Self-Archiving.

## University of Bath

### General rights

Copyright and moral rights for the publications made accessible in the public portal are retained by the authors and/or other copyright owners and it is a condition of accessing publications that users recognise and abide by the legal requirements associated with these rights.

### Take down policy

If you believe that this document breaches copyright please contact us providing details, and we will remove access to the work immediately and investigate your claim.

**N-Heterocyclic Carbene Non-Innocence in the Catalytic Hydrophosphination of  
Alkynes**

William J. M. Blackaby,<sup>[a]</sup> Samuel E. Neale,<sup>[b]</sup> Connie J. Isaac,<sup>[a]</sup> Sara Sabater,<sup>[a]</sup> Stuart A.  
Macgregor\*<sup>[b]</sup> and Michael K. Whittlesey\*<sup>[a]</sup>

[a] W. J. M. Blackaby, C. J. Isaac, Dr. S. Sabater, Prof. M. K. Whittlesey

Department of Chemistry

University of Bath

Claverton Down, Bath BA2 7AY, UK

E-mail: m.k.whittlesey@bath.ac.uk

[b] S. E. Neale, Prof. S. A. Macgregor

Institute of Chemical Sciences

Heriot-Watt University, Edinburgh, EH14 4AS, UK.

E-mail: S.A.Macgregor@hw.ac.uk

Corresponding author: Professor M. K. Whittlesey

## Abstract

Studies on alkyne hydrophosphination employing nickel-NHC catalysts (NHC = N-heterocyclic carbene) revealed that the free N-alkyl substituted NHCs themselves were catalytically active. DFT calculations showed the mechanism involves the NHC acting as a Brønsted base to form an imidazolium phosphide species which then undergoes rate-limiting nucleophilic attack at the terminal alkyne carbon. This mechanism explains the preference seen experimentally for reactions with aryl substituted phosphines and alkynes, while the rearrangements of the alkenyl anion formed upon P–C bond formation account for the observation of both *Z*- and *E*-regioisomers of the products.

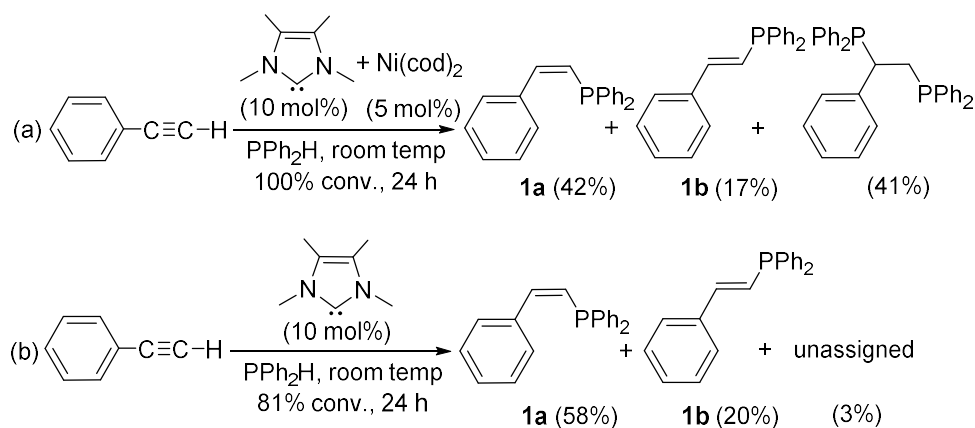
## Introduction

N-heterocyclic carbenes (NHCs) have proven to be highly effective ligands for the transition metal catalyzed addition of E–H groups (E = H, group 13-15 element) across unsaturated C–C bonds.<sup>[1]</sup> In such processes it is usually assumed that the NHC plays the role of a strongly bound ‘spectator’ ligand that remains coordinated to the metal center throughout the catalytic cycle. Moreover, even if dissociation of the NHC ligand were to take place, the lack of precedent for reactions of NHCs with E–H bonds, even under stoichiometric conditions,<sup>[2-5]</sup> would suggest the free carbenes would remain innocent and thus not contribute to catalysis.<sup>[6]</sup> Herein, we report an example that demonstrates this is not the case.

## Results and Discussion

During studies of P–H bond addition to alkynes (hydrophosphination) catalyzed by N-alkyl substituted NHC complexes of nickel (Scheme 1a),<sup>[7]</sup> control experiments demonstrated that catalysis also proceeded when only the NHC was present in the absence of any nickel. Thus, a 10 mol% loading of IMe<sub>4</sub> (for the structures of all of the carbenes used in this study, see Chart 1) gave 81% conversion of phosphine<sup>[8]</sup> to a 3.3:1 molar ratio of the *Z*- and *E*-anti-Markovnikov products **1a** and **1b** after 24 h at room temperature in THF (Scheme 1b).<sup>[9]</sup> The *Z*-product **1a** was also favoured in the Ni catalyzed reaction, although this also resulted in significant amounts of double hydrophosphination.

Other N-alkyl substituted NHCs proved to be equally adept at catalysis (Table 1, entries 1-5; ESI), yielding the *Z*-anti-Markovnikov product as the major isomer in the majority of cases. Neither unsaturated (entries 6, 7) nor saturated (entry 8) N-aryl substituted NHCs gave good catalytic activity. Both the diamidocarbene 6MesDAC (entry 9) and cyclic alkyl amino carbene <sup>Et</sup>2CAAC (entry 10) proved totally ineffective.



**Scheme 1.** Comparison of (a) Ni-NHC and (b) NHC-alone catalysed hydrophosphination of  $\text{PhC}\equiv\text{CH}$  with  $\text{PPh}_2\text{H}$ .

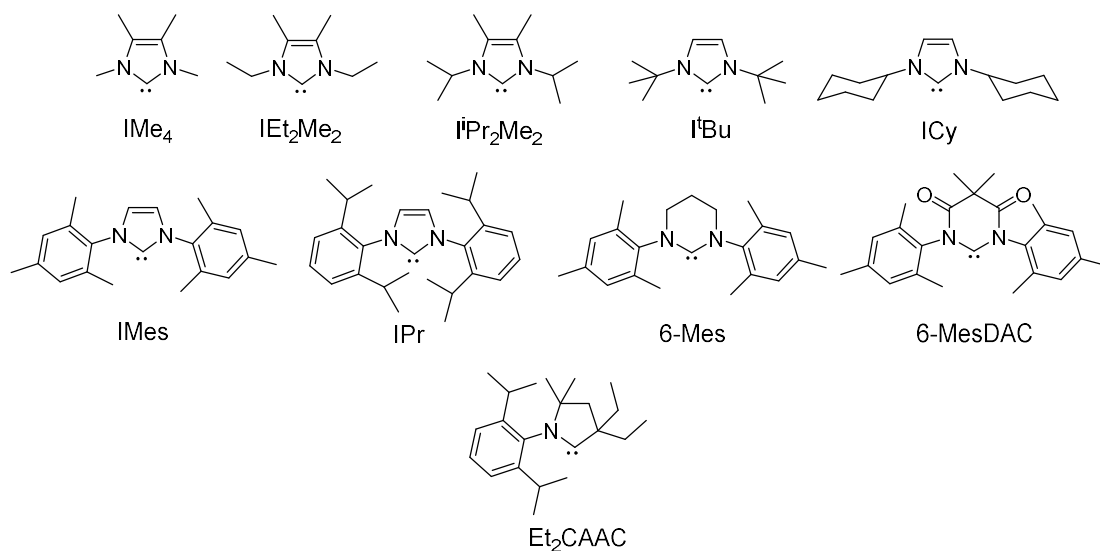


**Chart 1.** Structures and abbreviations of the carbenes used in this study.

The complete absence of side products seen with  $\text{I}^{\text{Bu}}$  (entry 4) led us to conduct more detailed investigations of the hydrophosphination reaction with this NHC. No reaction was observed with just  $\text{PhC}\equiv\text{CH}$  (10 equiv),<sup>[10]</sup> whereas treatment of the carbene with  $\text{PPh}_2\text{H}$  (10 equiv) resulted in formation of the aminal,  $\text{I}^{\text{Bu}}\text{H}_2$ ,<sup>[11]</sup> and the product of dehydrocoupling,<sup>[12]</sup>  $\text{Ph}_2\text{P}-\text{PPh}_2$ . NMR monitoring of a catalytic reaction of  $\text{PPh}_2\text{H}$  and  $\text{PhC}\equiv\text{CH}$  with 10 mol%  $\text{I}^{\text{Bu}}$  in THF as a function of time revealed that hydrophosphination was in fact very rapid,

with 78% consumption of the phosphine within 20 min. NMR spectroscopy showed that *t*Bu was still intact at the end of the catalytic run. Upon addition of further PPh<sub>2</sub>H and PhC≡CH, 70% of the phosphine was consumed within 1.5 h. Catalysis proved possible even at just 1 mol% *t*Bu, with 95% conversion of PPh<sub>2</sub>H taking place over ca. 2.5 days.

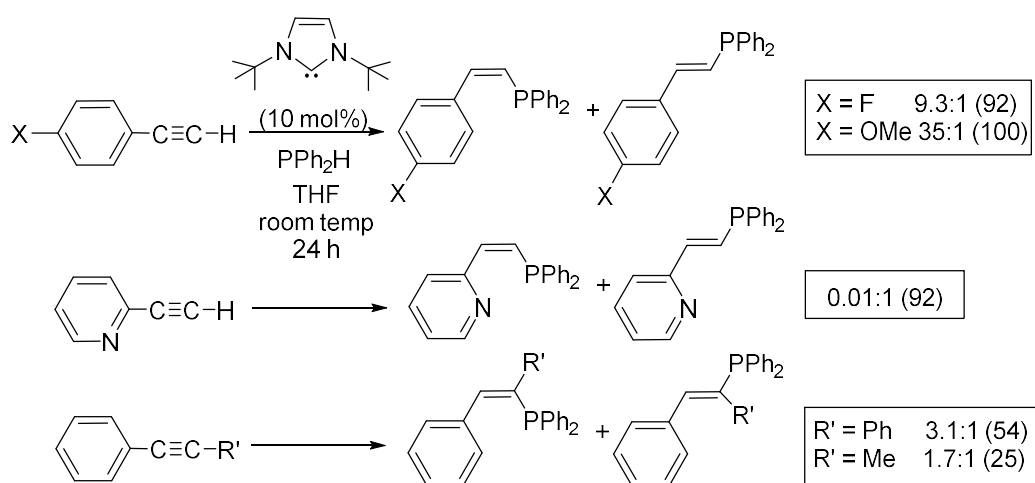
**Table 1.** NHC catalysed hydrophosphination of PhC≡CH with PPh<sub>2</sub>H.<sup>[a]</sup>

$$\text{Ph-C}\equiv\text{C-H} \xrightarrow[\text{PPh}_2\text{H}]{\text{carbene (10 mol\%)}} \text{Ph-CH=CH-PPh}_2 + \text{Ph-CH=CH-PPh}_2$$
 THF, room temp

Entry	Carbene	Conversion (%) of PPh <sub>2</sub> H	Hydrophosphination products (%) as percentage of all products	Z:E ratio
1	IMe <sub>4</sub>	81	90	2.8:1
2	IEt <sub>2</sub> Me <sub>2</sub>	92	74	0.9:1
3	<i>i</i> Pr <sub>2</sub> Me <sub>2</sub>	85	93	2.0:1
4	<i>t</i> Bu	89	100	3.5:1
5	ICy	92	100	2.6:1
6	IMes <sup>[c]</sup>	14	71	-[d]
7	IPr <sup>[c]</sup>	0	-	-
8	6-Mes <sup>[c]</sup>	9	100	-[d]
9	6MesDAC <sup>[c]</sup>	0	-	-
10	<sup>Et</sup> 2CAAC	6 <sup>[c]</sup>	0	-

<sup>[a]</sup>Conditions: Carbene (0.04 mmol), alkyne (0.40 mmol), PPh<sub>2</sub>H (0.44 mmol), THF (0.5 mL), room temperature. <sup>[b]</sup>Based on phosphine consumption as quantified by inverse-gated <sup>31</sup>P{<sup>1</sup>H} NMR spectra. <sup>[c]</sup>18 h reaction time. <sup>[d]</sup>Only the *Z*-isomer of PhCH=CH(PPh<sub>2</sub>) was formed. <sup>[e]</sup>Product of Ph<sub>2</sub>-H addition to CAAC formed.<sup>[3b]</sup>

To ascertain further details about the catalysis, the electronic properties of the alkyne were varied and shown to impact on the product *Z:E* ratios (see Scheme 2 and ESI). Both *para*-F and *para*-OMe substituents increased significantly the *Z:E* ratio (9:3:1 and 35:1 respectively), whereas the *ortho*-2-pyridyl-substituted substrate led to preferential generation of the *E*-isomer (*Z:E* = 0.01:1). The internal alkynes PhC≡CPh and PhC≡CMe proved to be reactive, but afforded significant amounts of dehydrocoupling. Only dehydrocoupling was observed with 1-hexyne.



**Scheme 2.** *t*Bu catalyzed hydrophosphination of alkynes with PPh<sub>2</sub>H. Numbers shown on the right give the ratio of *Z:E* isomers and (in parentheses) percentage conversion of PPh<sub>2</sub>H.

The mechanism of the *t*Bu catalyzed hydrophosphination of PhC≡CH with PPh<sub>2</sub>H was probed using DFT calculations, with optimizations performed in THF solvent with the TPSS functional and final energies computed with M05-2X.<sup>[13]</sup> Reaction of *t*Bu with PPh<sub>2</sub>H involves an initial adduct, **I**, at +6.0 kcal/mol from which phosphine deprotonation occurs through **TS(I-II)** at +18.1 kcal/mol. This forms a contact ion-pair, [*t*BuH][PPh<sub>2</sub>] (**II**, +4.9 kcal/mol), which accesses P–C bond formation via **TS(II-III)** at +17.9 kcal/mol to give **III**, the product of net carbene insertion into the P–H bond, at +9.1 kcal/mol. No direct pathway

for this insertion process could be characterised and, at least for this combination of substrates, the insertion product is thermodynamically less favoured than the ion-pair **II**. Both the ion-pair and insertion product are thermodynamically uphill with respect to free *t*Bu and PPh<sub>2</sub>H and this is consistent with their non-observation experimentally. They are, however, kinetically accessible.

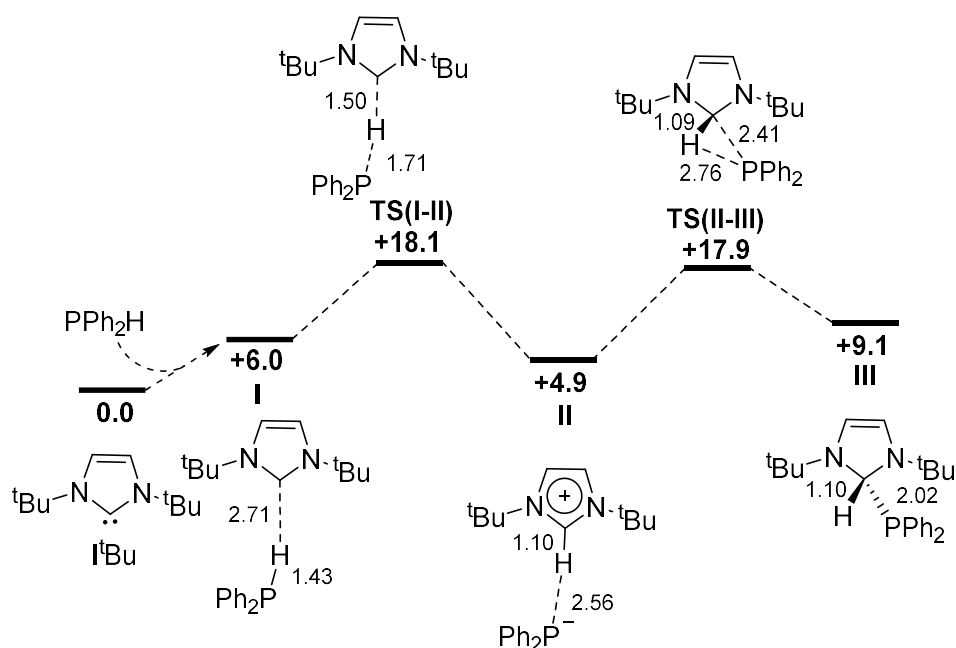


**Figure 1.** Computed free energy reaction profile for P-H activation of PPh<sub>2</sub>H with *t*BuI (kcal/mol, computed at the M052X-D3(THF)/def2-TZVP//TPSS(THF)DZP level).

The computed pathways for the onward reaction with phenylacetylene to form the *Z*- and *E*-isomers of PhCH=CH(PPh<sub>2</sub>) are shown in Figure 2 with details of key transition states in Figure 3. Initial nucleophilic attack of the phosphide ion within ion-pair **II** at the terminal alkyne carbon occurs via **TS(II-IV)** at +23.2 kcal/mol; the alternative attack at the internal carbon (that would lead to the Markovnikov product) involves a much less accessible transition state at 29.4 kcal/mol (see ESI). The new contact ion-pair formed, **IV** (+9.3 kcal/mol), comprises a *Z*-alkenyl anion and the imidazolium cation.



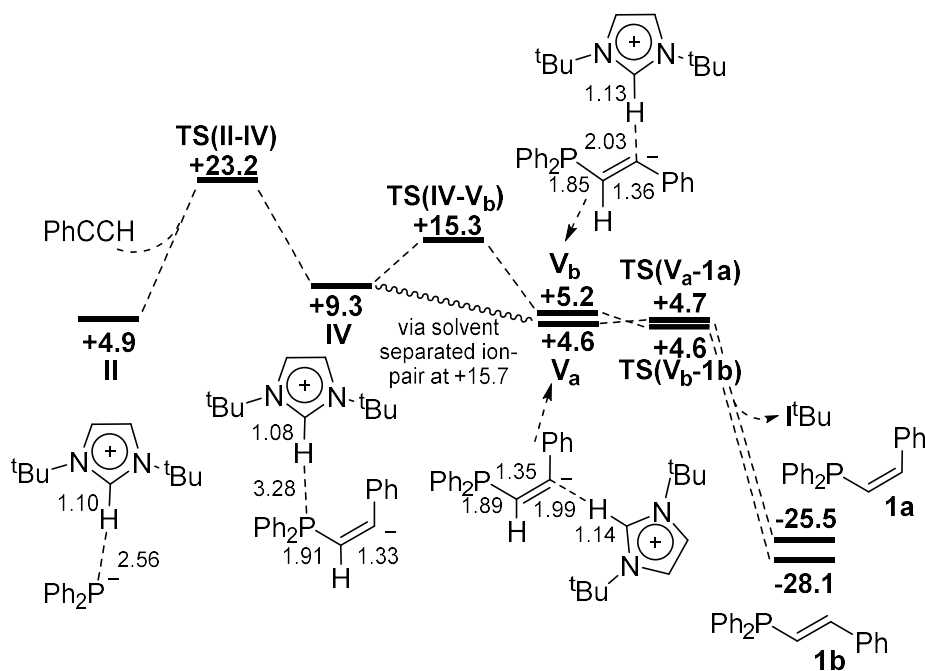


**Figure 2.** Computed free energy reaction profiles for formation of *Z*- and *E*-PhCH=CH(PPh<sub>2</sub>) via reaction of contact ion-pair **II** with PhC≡CH (kcal/mol computed at the M052X-D3(THF)/def2-TZVP//TPSS(THF)DZP level)

Formation of **1a** then requires movement of the imidazolium to place the C2–H bond adjacent to the alkenyl anion lone pair; this is most simply modelled by dissociation to a solvent-separated ion-pair at +15.7 kcal/mol which then recombines to give **V<sub>a</sub>** at +4.6 kcal/mol. Proton transfer within **V<sub>a</sub>** readily occurs to form **1a** and free *t*BuI at -25.5 kcal/mol. Alternatively, isomerization of **IV** can occur via an allenyl transition state structure **TS(IV-V<sub>b</sub>)** at 15.3 kcal/mol (Figure 3). This generates contact ion-pair **V<sub>b</sub>** at +4.6 kcal/mol with facile proton transfer then forming the *E*-isomer **1b** and *t*BuI at -28.1 kcal/mol.<sup>[14]</sup>

Combining Figures 1 and 2 shows hydrophosphination to be strongly exergonic ( $\Delta G = -25.5$  and  $-28.1$  kcal/mol for **1a** and **1b** respectively) and to have a reasonable overall barrier of 23.2 kcal/mol in which phosphide nucleophilic attack is rate-limiting. The geometry of **TS(II-IV)** (Figure 3, in which the imidazolium cation is omitted for clarity) shows developing *sp*<sup>2</sup>-character at both alkyne carbons and during this process (and ultimately in

intermediate **IV**), a formal negative charge developing on the  $\beta$ -carbon (with respect to  $\text{PPh}_2$ ) can be stabilised via delocalization around the adjacent phenyl ring. This accounts for the lack of hydrophosphination seen with 1-hexyne; indeed, the transition state computed using propyne as a model aliphatic alkyne is much higher in energy at +31.5 kcal/mol. With  $\text{PhC}\equiv\text{CMe}$ , an overall barrier of 29.0 kcal/mol is computed, consistent with the much lower reactivity of this substrate compared to  $\text{PhC}\equiv\text{CH}$  and presumably reflecting the greater steric encumbrance associated with attack at an internal alkyne carbon. Details of all additional pathways are provided in the ESI.

Based on these computed profiles, the ratio of the hydrophosphination products, **1a:1b**, will be determined by the rates of the different rearrangements of intermediate **IV**. While formation of **V<sub>b</sub>** is well-defined via **TS(IV-V<sub>b</sub>)** at 15.3 kcal/mol, it is less straightforward to assess the formation of **V<sub>a</sub>**. In Figure 2 this is assumed to proceed via a solvent-separated ion-pair at 15.7 kcal/mol, but other possibilities can be considered, including rearrangement within the contact ion-pair, or addition of a second, external imidazolium cation directly to the alkenyl carbon. As such, 15.7 kcal/mol may be considered as an upper limit for this rearrangement barrier. The two processes leading to **1a** and **1b** are therefore likely to be competitive, and indeed experimentally both isomers are observed in most cases (Scheme 2). Recomputing these rearrangements with  $p\text{-XC}_6\text{H}_4\text{C}\equiv\text{CH}$  ( $X = \text{F}, \text{OMe}$ ) shows the separated ion-pair becomes more accessible than the isomerization via **TS(IV-V<sub>b</sub>)**: for  $X = \text{F}$  the ion-pair is 1.1 kcal/mol more stable (+15.3 kcal/mol *cf.* +16.4 kcal/mol), while for  $X = \text{OMe}$  the difference increases to 2.0 kcal/mol (ion-pair: +19.2 kcal/mol; **TS(IV-V<sub>b</sub>)**: +21.2 kcal/mol). Formation of **V<sub>a</sub>** (and hence the *Z*-isomer **1a**) therefore becomes more favored with these substituted alkynes, reflecting the higher *Z:E*-ratios observed experimentally. NBO charge calculations on **TS(IV-V<sub>b</sub>)** indicate an increase in negative charge in the aryl substituent that appears to be poorly accommodated by +M substituents. In contrast, +I substituents would be

expected to facilitate isomerization and lead to lower *Z*:*E* ratios. This is confirmed with calculations on *p*-CF<sub>3</sub>C<sub>6</sub>H<sub>4</sub>C≡CH for which the isomerization transition state was computed to lie 5.1 kcal/mol below the solvent-separated ion-pair (see ESI) indicating the *E*-isomer should be preferred.<sup>[15]</sup> This was subsequently borne out experimentally with the *t*Bu-catalyzed hydrophosphination of this substrate giving exclusively the *E*-isomer of *p*-CF<sub>3</sub>C<sub>6</sub>H<sub>4</sub>CH=CH(PPh<sub>2</sub>) (ESI).

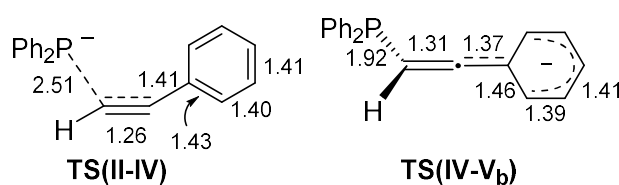


**Figure 3.** Computed geometries for key transition states **TS(II-IV)** and **TS(IV-V<sub>b</sub>)**. Selected distances are given in Å and spectator imidazolium cations have been omitted for clarity.

Hydrophosphination with a simple dialkylphosphine, PMe<sub>2</sub>H, with PhC≡CH was also modeled. As for PPh<sub>2</sub>H, insertion of *t*Bu into the P–H bond involves a two-step process via a contact ion-pair; however in this case the neutral carbene insertion product (**III**<sub>Me</sub>, +7.0 kcal/mol) is now significantly more stable than the preceding ion-pair (**II**<sub>Me</sub>, +22.2 kcal/mol). Onward reaction of **II**<sub>Me</sub> with PhC≡CH entails a transition state at +35.1 kcal/mol. This reflects the lack of reactivity observed experimentally upon replacing PPh<sub>2</sub>H with *t*Bu<sub>2</sub>H (ESI) and correlates with the much higher *p*K<sub>a</sub> of dialkyl- versus diaryl-phosphines.<sup>[16]</sup>

In conclusion, we have shown that N-alkyl substituted NHCs can promote the catalytic hydrophosphination of alkynes. The proposed mechanism (Figures 1 and 2) indicates that initial P–H activation proceeds via deprotonation with the NHC acting as a Brønsted base. P–C bond formation involves rate-limiting nucleophilic attack of the resultant phosphide at the

more accessible alkyne carbon, with *Z:E* selectivity being determined by the rearrangements of the resultant alkenyl anion. This mechanism accounts for the scope of the reaction which favors relatively acidic arylphosphines, as well as aryl-substituted alkynes in which charge delocalization around the aryl ring provides additional stabilization of the alkenyl anion intermediate. This catalytic hydrophosphination has parallels to NHC-catalyzed conjugate addition reactions in which the NHC acts as a general base to activate alcohols, amines and ketones.<sup>[17]</sup>

While examples of base-catalyzed hydrophosphination have previously been reported,<sup>[18,19]</sup> these typically employ more explicit bases such as KO<sup>t</sup>Bu or KHMDS.<sup>[20]</sup> In contrast, in catalysis with transition metal-NHC complexes, the role of the NHC is usually assumed to be as a ligand, but this study shows that the capability of any dissociated, free NHC to act as a base and perform catalysis in its own right should not necessarily be neglected. Finally, it is interesting that the catalytic alkyne hydrophosphination reported herein does not rely on E–H bond ‘oxidative addition’ (i.e. carbene insertion) of the type often targeted in putative main group catalysis.<sup>[21]</sup> While we compute such species to be kinetically accessible, in the present case they lie off-cycle and thus do not contribute directly to catalysis.

## Acknowledgements

We thank the EPSRC (Doctoral Training Award for WJMB), Heriot-Watt University (James Watt Scholarship for SEN) and Royal Society (Newton Fellowship to SS) for financial support. Drs. Ruth Webster, James Taylor and David Carbery (all University of Bath) are thanked for valuable discussions, and Dr. Rodolphe Jazzar (UC San Diego) is acknowledged for the gift of <sup>Et2</sup>CAAC.

## References

- [1] a) *N-Heterocyclic Carbenes: Effective Tools for Organometallic Synthesis* (Ed.: S. P. Nolan), Wiley-VCH, Weinheim, 2014; b) *N-Heterocyclic Carbenes: From Laboratory Curiosities to Efficient Synthetic Tools* (Ed.: S. Díez-González), 2nd Ed., RSC, Cambridge, 2017.
- [2] H. Song, Y. Kim, J. Park, K. Kim, E. Lee, *Synlett* **2016**, 27, 477-485.
- [3] For specific examples of stoichiometric E-H activation with NHCs, see: a) A. J. Arduengo III, J. C. Calabrese, F. Davidson, H. V. Rasika Dias, J. R. Goerlich, R. Krafczyk, W. J. Marshall, M. Tamm, R. Schmutzler, *Helv. Chim. Acta* **1999**, 82, 2348-2364; b) G. D. Frey, J. D. Masuda, B. Donnadieu, G. Bertrand, *Angew. Chem.* **2010**, 122, 9634-9637; *Angew. Chem. Int. Ed.* **2010**, 49, 9444-9447; c) M. Bispinghoff, A. M. Tondreau, H. Grützmacher, C. A. Faradji, P. G. Pringle, *Dalton Trans.* **2016**, 45, 5999-6003.
- [4] E-H bond activation is also implicit in borane and silane induced ring expansions of NHCs. a) D. Schmidt, J. H. J. Berthel, S. Pietsch, U. Radius, *Angew. Chem.* **2012**, 124, 9011-9015; *Angew. Chem. Int. Ed.* **2012**, 51, 8881-8885; b) S. Würtemberger-Pietsch, H. Schneider, T. B. Marder, U. Radius, *Chem. Eur. J.* **2016**, 22, 13032-13036.
- [5] a) For examples of E-H activation with other types of heterocyclic carbenes, see: a) G. D. Frey, V. Lavallo, B. Donnadieu, W. W. Schoeller, G. Bertrand, *Science* **2007**, 316, 439-441; b) Ref 3b; c) T. W. Hudnall, J. P. Moerdyk, C. W. Bielawski, *Chem. Commun.* **2010**, 46, 4288-4290; d) D. T. Chase, J. P. Moerdyk, C. W. Bielawski, *Org. Lett.* **2014**, 16, 812-815; e) J. Auth, J. Padevet, P. Mauleón, A. Pfaltz, *Angew. Chem. Int. Ed.* **2015**, 127, 9678-99681; *Angew. Chem. Int. Ed.* **2015**, 54, 9542-9545; f) J. Auth, J. Padevet, P. Mauleón, A. Pfaltz, *Angew. Chem. Int. Ed.* **2017**, 129, 9394-9394;

- Angew. Chem. Int. Ed.* **2017**, *56*, 9266-9266; g) Z. R. Turner, *Chem. Eur. J.* **2016**, *22*, 11461-11468; h) U. S. D. Paul, U. Radius, *Chem. Eur. J.* **2017**, *23*, 3993-4009.
- [6] a) O. Jacquet, C. D. Gomes, M. Ephritikhine, T. Cantat, *J. Am. Chem. Soc.* **2012**, *134*, 2934-2937; b) Q. Zhou, Y. Li, *J. Am. Chem. Soc.* **2015**, *137*, 10182-10189.
- [7] S. Sabater, M. J. Page, M. F. Mahon, M. K. Whittlesey, *Organometallics* **2017**, *36*, 1776-1783.
- [8] In all cases, the phosphine products were not isolated. Conversions were determined by inverse-gated  $^{31}\text{P}\{^1\text{H}\}$  NMR spectroscopy, following the work by Oro and co-workers. A. Di Giuseppe, R. De Luca, R. Castarlenas, J. J. Pérez-Torrente, M. Crucianelli, L. A. Oro, *Chem. Commun.* **2016**, *52*, 5554-5557.
- [9] The *Z:E* ratio was unchanged when catalytic reactions with  $\text{IMe}_4$  were performed in toluene, benzene or cyclohexane, although conversions (72, 46 and 55% respectively) were lower than in THF.
- [10] In the case of  $\text{IMe}_4$ , addition of  $\text{PhC}\equiv\text{CH}$  (10 equiv, THF) led to the instantaneous appearance of a  $^1\text{H}$  NMR spectrum (ESI) suggestive of the formation of the addition product  $(\text{IMe}_4)(\text{C}\equiv\text{CPh})\text{H}$  ( $\delta = 3.76$  ppm (1H), 2.44 ppm (6H), 1.63 ppm (6H)).<sup>[3a,5g]</sup> However, this species decomposed in solution overnight. Additional characterisation is the subject of ongoing studies.
- [11] H. Schneider, D. Schmidt, U. Radius, *Chem. Commun.* **2015**, *51*, 10138-10141.
- [12] A. Jana, C. Schulzke, H. W. Roesky, *J. Am. Chem. Soc.* **2009**, *131*, 4600-4601.
- [13] Calculations employed Gaussian 09. Geometries were optimised with the TPSS functional using a double- $\xi$  plus polarization basis set and included the effects of THF solvent within the optimization protocol. All stationary points were characterised via frequency calculations and these also provided thermal and entropic corrections. Energies were then re-computed with the M05-2X functional with a def2TZVP basis

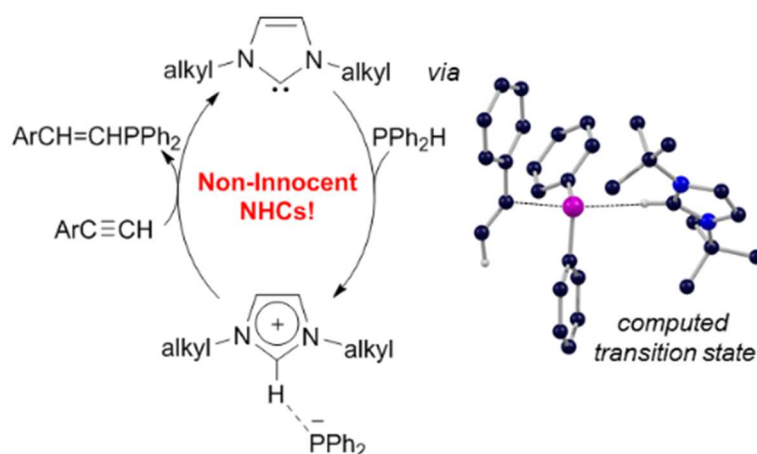
set and including corrections for dispersion (D3) and THF solvent. Final energies quoted in the text are free energies. See ESI for full details.

- [14] Attempts to characterise an alternative pathway involving nucleophilic attack of the phosphorus lone pair in the neutral carbene insertion intermediate **III** were unsuccessful with all structures reverting to ion-pair **II**.
- [15] Attempts to model these pathways for 2-C<sub>5</sub>H<sub>5</sub>N-C≡CH (for which the *E*-isomer is strongly favoured) were complicated by the presence of H-bonding to the free pyridyl nitrogen.
- [16] J.-N. Li, L. Liu, Y. Fu, Q.-X. Guo, *Tetrahedron* **2006**, *62*, 4453–4462.
- [17] a) S. J. Ryan, L. Candish, D. W. Lupton, *Chem. Soc. Rev.* **2013**, *42*, 4906-4917; b) D. M. Flanigan, F. Romanov-Michailidis, N. A. White, T. Rovis, *Chem. Rev.* **2015**, *115*, 9307-9387; c) N. Wang, J. H. Xu, J. K. Lee, *Org. Biomol. Chem.* **2018**, *16*, 6852-6866.
- [18] a) J. L. Bookham, D. M. Smithies, *J. Organomet. Chem.* **1999**, *577*, 305-315; b) T. Bunlaksananusorn, P. Knochel, *Tetrahedron Lett.* **2002**, *43*, 5817-5819; c) O. Delacroix, A. C. Gaumont, *Curr. Org. Chem.* **2005**, *9*, 1851-1882; d) S. N. Arbuzova, N. K. Gusarova, B. A. Trofimov, *ARKIVOC* **2006**, 12-36; e) A. Perrier, V. Comte, C. Moïse, P. Richard, P. Le Gendre, *Eur. J. Org. Chem.* **2010**, 1562-1568; f) N. T. Coles, M. F. Mahon, R. L. Webster, *Chem. Commun.* **2018**, *54*, 10443-10446
- [19] Solvent and catalyst-free alkyne hydrophosphination has also been described, although forcing conditions are necessary. Y. Moglie, M. J. González-Soria, I. Martín-García, G. Radivoy, F. Alonso, *Green. Chem.* **2016**, *18*, 4896-4907.
- [20] For a direct comparison to the NHC catalysed reactions, the hydrophosphination of PhC≡CH with PPh<sub>2</sub>H using KHMDS and KO<sup>t</sup>Bu as catalysts was performed under the same conditions employed in Table 1. In both cases, complete consumption of the

phosphine took place in ca. 15 min, to afford a 1.2:1 and 1.7:1 ratio of *E*:*Z* isomers respectively. Over longer times (ca. 4 h), this ratio changed to 0.1:1 (KHMDS) and 0.94:1 (KO<sup>t</sup>Bu).

- [21] a) P. P. Power, *Nature* **2010**, *463*, 171-177; b) K. Revunova, G. I. Nikonov, *Dalton Trans.* **2015**, *44*, 840-866; c) S. Inoue, C. Weetman, *ChemCatChem* **2018**, *10*, 4213-4228; d) T. Chu, G. I. Nikonov, *Chem. Rev.* **2018**, *118*, 3608-3680.

### Table of Contents Entry



Free N-alkyl substituted N-heterocycle carbenes (NHCs) promote the catalytic hydrophosphination of aryl-substituted alkynes through a mechanism involving nucleophilic attack of an imidazolium phosphide species at the terminal alkyne carbon. These results highlight the potential non-innocence of NHCs in their use as ligands in metal catalysed transformations.